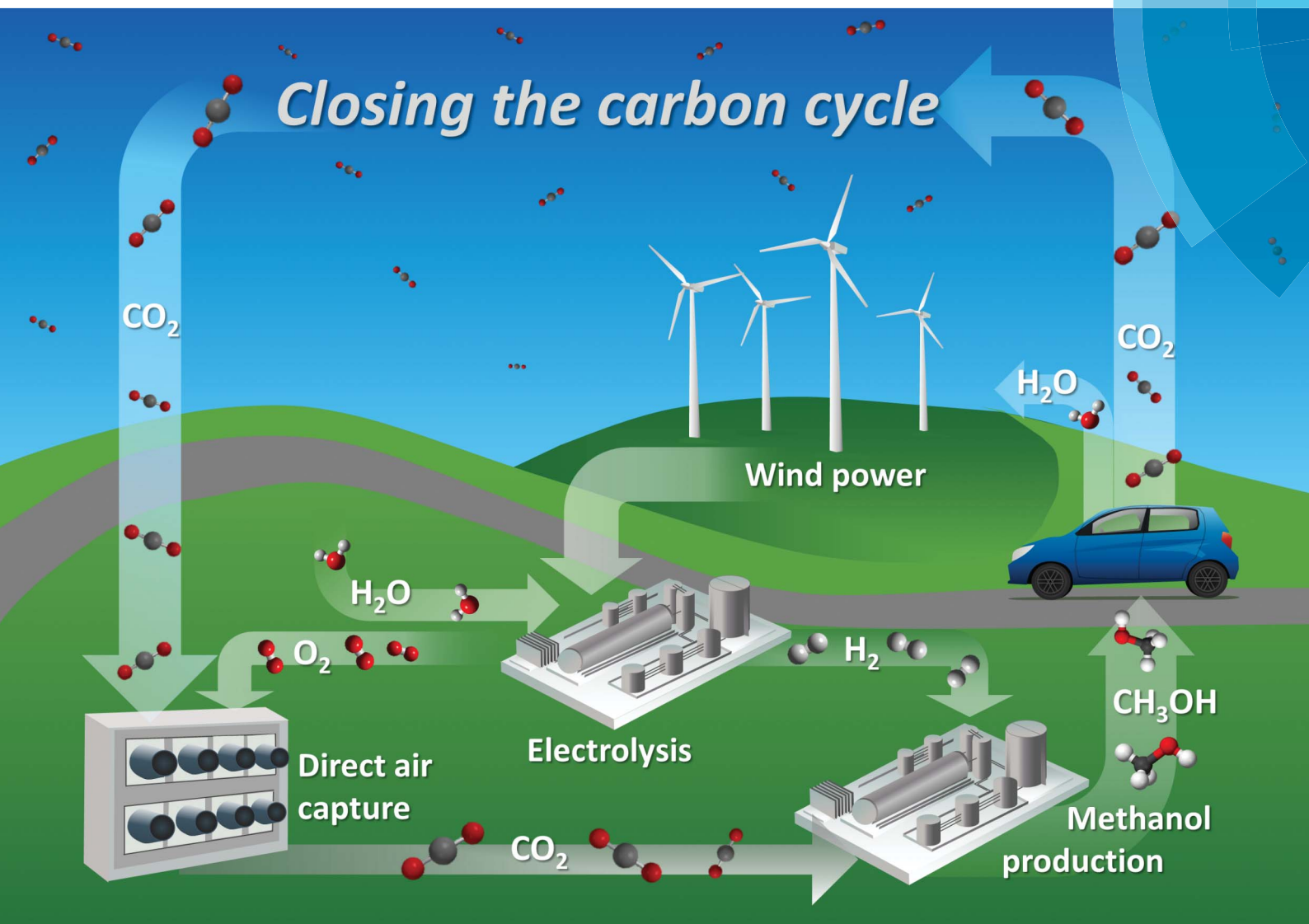


Sustainable Energy & Fuels

Interdisciplinary research for the development of sustainable energy technologies
rsc.li/sustainable-energy



ISSN 2398-4902



PAPER

Niall Mac Dowell et al.

Closing the carbon cycle to maximise climate change mitigation:
 power-to-methanol vs. power-to-direct air capture



Cite this: *Sustainable Energy Fuels*, 2018, 2, 1153

Closing the carbon cycle to maximise climate change mitigation: power-to-methanol vs. power-to-direct air capture

H. A. Daggash, C. F. Patzschke, C. F. Heuberger, L. Zhu, K. Hellgardt, P. S. Fennell, A. N. Bhave, A. Bardow and N. Mac Dowell

It is broadly recognised that CO₂ capture and storage (CCS) and associated negative emissions technologies (NETs) are vital to meeting the Paris agreement target. The hitherto failure to deploy CCS on the required scale has led to the search for options to improve its economic return. CO₂ capture and utilisation (CCU) has been proposed as an opportunity to generate value from waste CO₂ emissions and improve the economic viability of CCS, with the suggestion of using curtailed renewable energy as a core component of this strategy. This study sets out to quantify (a) the amount of curtailed renewable energy that is likely to be available in the coming decades, (b) the amount of fossil CO₂ emissions which can be avoided by using this curtailed energy to convert CO₂ to methanol for use as a transport fuel – power-to-fuel, with the counterfactual of using that curtailed energy to directly remove CO₂ from the atmosphere via direct air capture (DAC) and subsequent underground storage, power-to-DAC. In 2015, the UK curtailed 1277 GWh of renewable power, or 1.5% of total renewable power generated. Our analysis shows that the level of curtailed energy is unlikely to increase beyond 2.5% until renewable power accounts for more than 50% of total installed capacity. This is unlikely to be the case in the UK before 2035. It was found that: (1) power-to-DAC could achieve 0.23–0.67 t_{CO₂} avoided MWh⁻¹ of curtailed power, and (2) power-to-fuel could achieve 0.13 t_{CO₂} avoided MWh⁻¹. The power-to-fuel concept was estimated to cost \$209 t_{CO₂} avoided⁻¹ in addition to requiring an additional \$430–660 t_{CO₂} avoided⁻¹ to finally close the carbon cycle by air capture. The power-to-DAC concept was found to cost only the \$430–660 t_{CO₂} avoided⁻¹ for air capture. For power-to-fuel to become profitable, hydrogen prices would need to be less than or equal to \$1635 t_{H₂} avoided⁻¹ or methanol prices must increase to \$960 t_{MeOH} avoided⁻¹. Absent this change in H₂ price or methanol value, a subsidy of approximately \$283 t_{CO₂} avoided⁻¹ would be required. A core conclusion of this study is that using (surplus) renewable energy for direct air capture and CO₂ storage is a less costly and more effective option to mitigate climate change than using this energy to produce methanol to substitute gasoline.

Received 9th February 2018
Accepted 13th March 2018

DOI: 10.1039/c8se00061a
rsc.li/sustainable-energy

1 Introduction

Whilst the 2015 Paris agreement symbolised the recognition of climate change as a global issue and achieved political

consensus to limit its consequences, mainstream climate policy is yet to evolve to promote the proposed mitigation strategies required to achieve the agreed well below 2 °C warming (above pre-industrial levels) target. Integrated assessment models (IAMs) are reliant on the deployment of CCS and negative emissions technologies (NETs) to meet this target.^{1–6} Despite the prevalence of CCS in all mitigation pathways compliant with the Paris target, high investment and operating costs, and cross-chain risks have deterred its deployment at the required scale.^{7,8} An absence of financial incentives, policy drivers and/or political appetite has compounded the investment challenges of developing CCS infrastructure. These challenges have driven the search for means to improve the economic viability of CCS, one of which is carbon dioxide (CO₂) capture and utilisation (CCU).^{9,10}

The appeal of CCU lies in its alleged potential to valorise CO₂ by converting waste emissions into valuable products. CCU comprises both capture processes from industrial and diffuse

^aGrantham Institute for Climate Change and the Environment, Imperial College London, Exhibition Road, London, SW7 2AZ, UK

^bCentre for Environmental Policy, Imperial College London, Exhibition Road, London, SW7 2AZ, UK. E-mail: niall@imperial.ac.uk; Tel: +44 (0)20 7594 9298

^cCentre for Process Systems Engineering, Imperial College London, Exhibition Road, London, SW7 2AZ, UK

^dDepartment of Chemical Engineering, Imperial College London, Exhibition Road, London, SW7 2AZ, UK

^eCMCL, Salisbury House, Station Road, Cambridge, CB1 2LA, UK

^fLehrstuhl für Technische Thermodynamik, RWTH Aachen University, 52062 Aachen, Germany

† Currently visiting the Department of Chemical and Biological Engineering, University of British Columbia, Vancouver, Canada.

‡ These authors supervised the analysis.



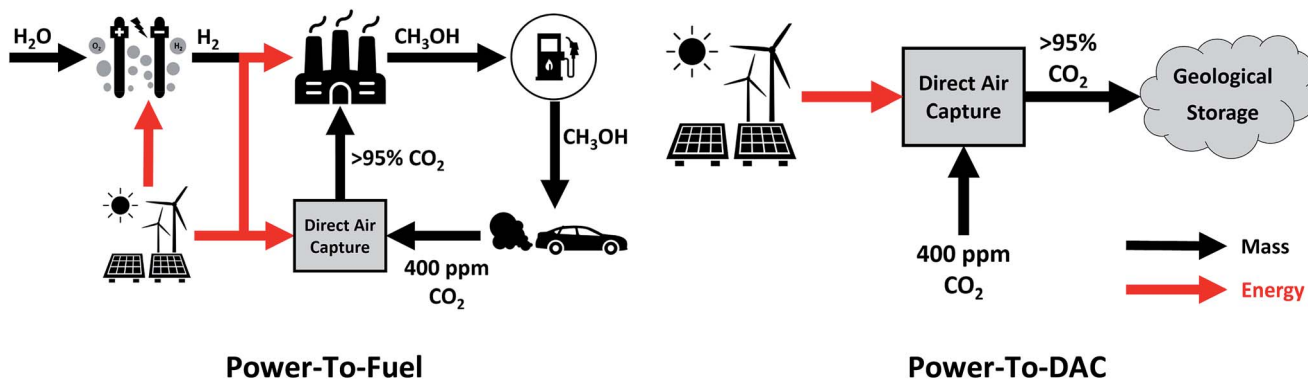


Fig. 1 Conceptual diagrams of the proposed circular economy of power-to-Fuel (left) and power-to-DAC (right) processes.

CO_2 sources, and their direct or indirect utilisation. Approximately 0.5% of global CO_2 emissions is currently utilised, mostly for enhanced oil recovery (EOR) or the synthesis of urea and speciality chemicals.^{11,12} Some routes for CO_2 utilisation are currently commercialised, such as CO_2 -based polymers.¹³ It is further argued that CCU could serve to make CCS more financially attractive by offsetting investment costs with revenue from CO_2 -derived products.¹³

Decarbonising the transport sector, which accounts for approximately 14% of total anthropogenic GHG emissions, is considered difficult because of the multitude of small, mobile emitters.¹ Additionally, with global fuel consumption two orders of magnitude higher than that of chemicals, CCU for the production of transport fuels has been promoted as providing an attractive opportunity for simultaneous value creation and emissions reduction.^{7,14} Moreover, owing to the increasing deployment of intermittent renewable energy sources, it is argued that renewable energy that would otherwise be curtailed can be used to operate these CCU processes, with this energy, available at zero or even negative cost.¹⁵

This study sets out to quantify: (a) the amount of curtailed renewable energy that is likely to be available in the medium term, (b) the extent to which transport-related CO_2 emissions can be avoided *via* a power-to-fuel strategy, and (c) to contrast this with the counterfactual argument of using the otherwise curtailed renewable energy to directly remove CO_2 from the atmosphere *via* a direct air capture (DAC) process. The power-to-fuel scenario utilises curtailed renewable electricity to produce H_2 which is subsequently reacted with CO_2 to produce methanol as a gasoline substitute. The CO_2 emissions from the methanol-powered cars are recycled for the continued production of methanol *via* direct air capture (DAC). In contrast, power-to-DAC uses the electricity to operate a DAC plant which directly removes CO_2 from the atmosphere; the captured CO_2 is then permanently sequestered. Both process are illustrated in Fig. 1.

2 Key enabling factors

2.1 Curtailed renewable energy

While CCS deployment has, as yet, failed to materialise at scale, mitigation efforts have, however, resulted in an

increasing penetration of renewables into the electricity system. The relative unpredictability of their supply poses risks to grid stability and reliability, and their increased deployment may see a manifestation of those risks.¹⁶ The various technical requirements for grid stability and security of supply are discussed elsewhere,¹⁷ and are not repeated here. Surplus generation during low-demand hours and full storage capacity, coupled with the difficulty of rapidly ramping (up or down) firm low-carbon electricity generation will likely see an increase in constraint payments already made to wind farms to curtail their generation. The opportunity for developing CO_2 utilisation processes using surplus electricity from intermittent renewables energy sources (iRES) depends on the quantity of this surplus, which is spatially and temporally varying. It is therefore helpful to review recent experience with curtailment of power generation from iRES in various power systems and curtailment analyses with energy system models.

Public and research literature do not provide a unique definition for curtailment in power systems. Curtailment levels are reported as the amount of downwards regulated power from iRES[§] per maximum potential power generation from iRES,¹⁸ per total system-wide power generation, or per total electricity demand.¹⁹ These different definitions lead to different numerical value, hence curtailment levels should be compared with caution.

Curtailment of power generation from iRES is a security measure required to maintain power system stability and operability, and to prevent equipment damage.²⁰ The reasons for curtailment depend on the specific conditions of a given network with regards to generation, energy storage, and transmission capacity.²¹ Often a surplus of power generation from iRES or conventional units during periods of low demand is the cause, but prevention or mitigation of transmission congestion (*e.g.*, in the United States (US) MISO network) and/or initial lack of transmission capacity (*e.g.*, China, US ERCOT) may make curtailment necessary.^{18,22} As observed in the Irish power system, exogenous operating

[§] Available power not generated or not supplied to transmission grid.



requirements, *e.g.*, a minimum share of firm reserve capacity, ¶ can also result in curtailment of power generation from iRES.¹⁸

iRES are near-zero marginal cost units, consequently, reduced generation (because of curtailment) is accompanied by a cost increase for electricity (per MWh).²² However, certain levels of curtailment can be economically sensible, reducing start-up cost and cycling for conventional power plants, or costly balancing mechanisms for transmission system operation. A dynamic system-wide economic dispatch assessment is necessary to evaluate the most economical and technically feasible operational strategy.²³

The analysis of historic power system data reveals curtailment levels of below 10% up to iRES penetration levels of 50% (as a percentage of available iRES power generation) in the UK, Ireland, and other European countries. A few sources report levels up to 20% at penetration levels exceeding 60%.²² In some US and Chinese power networks higher curtailment levels are observed, increasing above 20% at iRES penetration levels below 10%. Bird *et al.*, however, show that such historically high levels in the US were due to transmission bottlenecks and have since fallen to a range between 2–4%.¹⁸ The review¹⁸ presents a study of wind curtailment levels and causes across Europe, China, and the US for 2013 reports an overall average range of 1–3%. Where renewable energy is curtailed, those generators who are being constrained off the grid are compensated for this. For example, during Easter 2016, a total of \$5.3 million was paid to 39 UK wind farms, with constraint prices at \$83–225 MWh⁻¹.||**²⁵ Therefore, it is unlikely that this energy will be available at zero or negative cost to those wishing to use it.

Reduced incidences of curtailment can be achieved through increased power system flexibility, *e.g.*, through increased energy storage capacity or an expansion/reinforcement of the existing transmission grid. Changes in the electricity market and regulatory frameworks, as well as improved forecasting and dispatch strategies can equally alleviate high curtailment levels.¹⁸ The participation of iRES power generation units in ancillary services provides additional integration potential. The provision of upward reserve service requires large amounts of iRES power to be curtailed pre-emptively, which is not attractive under current market schemes.²⁶ However, the provision of downward reserve as well as voltage control in the case of wind power plants is technically possible and meaningful where market incentives are given. Additionally, if wind farms operate in a coordinated way, they may have the potential to provide secondary frequency control and so further reduce curtailment levels.²⁶

¶ System Non-Synchronous Penetration (SNSP) is the ratio of non-synchronous generation (wind and HVDC imports) to demand including HVDC exports. This limit is set to 50% in the Irish power grid in order to maintain grid stability and operability.

|| Using March 2016 exchange rate of \$1.4318 per £.

** In Germany, negative costs are currently paid due to policies enforcing the grid operations to feed in renewables. However, the hours with negative costs have been reducing in 2016 as well as the average negative cost.²⁴

Besides the analysis of real-word data, the energy systems modelling community has been studying curtailment in current and future power systems. A detailed study of the European electricity system including energy storage capacity expansion as well as transmission grid re-enforcement with the ReMix model reveals that even at penetration levels of 40–50% of iRES capacity not more than 1% of annual power demand is curtailed.¹⁹ As the iRES share increases to 60%, curtailment levels remain below 25% of annual power demand. It is observed that curtailment levels increase more rapidly in solar-dominated power systems. The PLEXOS model has been used to explore wind curtailment in a potential 2020 Irish power system.²⁷ The study reports transmission constraints as the primary driver of curtailment and finds a reduction in curtailment levels from 14 to 7% as reserve requirements (SNSP) are adjusted. Several measures are being pursued to minimise curtailment in regional power systems: automatic generation control²⁸ and expansion of the energy imbalance market,²⁹ amongst others, in California; grid expansion and award of priority to clean power feed in China;³⁰ flexibilisation of conventional power plants and expansion of regional transmission networks in Denmark;³¹ etc. These will serve to keep curtailment at or below contemporary levels. Thus, whilst it is evident that instances of surplus renewable energy have existed in different regions, going forward, curtailment is likely to be reduced.

We now present an iRES power curtailment analysis with the Electricity Systems Optimisation (ESO) modelling framework.²³ The ESO model is a hybrid capacity expansion and unit commitment model based on a total cost minimising mixed-integer linear program. The ESO model determines the optimal dispatch strategy on a hourly scale for one year without foreknowledge. The high temporal resolution combined with the detailed unit-wise representation of thermal, iRES, and energy storage technologies makes the ESO model well suited for analysis. As the national transmission grid is not considered in this model, the derived curtailment levels are due to demand-supply imbalances, technical operational constraints, and ancillary service constraints. The ESO model is parametrised to the power systems of the United Kingdom (UK) based on projections for 2030.³²

Similarly to previous studies, the analysis with the ESO model confirms low levels of curtailment of power generation from iRES as percentage of available iRES power generation at iRES penetration levels below 40%. Fig. 2 illustrates iRES power curtailment as a function of their penetration as output from the ESO model. We find that only at penetration levels above 50–60% do curtailment levels of greater than 2.5% occur. In a UK context, these values convert to an annual total of 11–77 TWh, approximately 3–19% of electricity demand in 2030. Based on BEIS' reference scenario and the CCC's central scenario of the UK's electricity generation mix, it is unlikely that the share of intermittent renewables will reach such levels by 2035.^{38,39}

Fig. 3 explores the optimal dispatch strategy for two sample days in the 2030 UK power system as determined with the ESO model. We can follow the individual power unit operation, storage charging and discharging, shown here aggregated by fuel type. In the 24 hour sequence on the left hand-side, no iRES



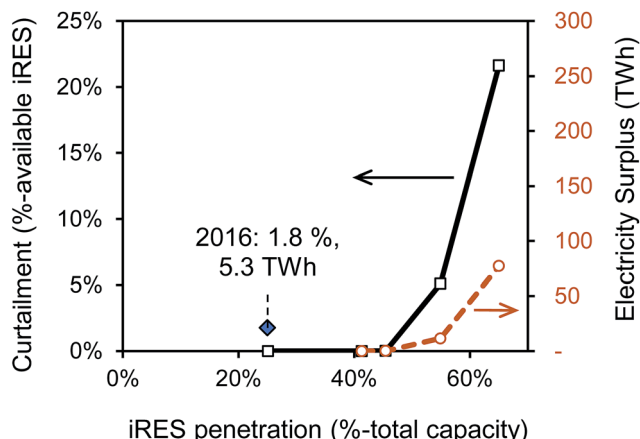


Fig. 2 Curtailment of intermittent renewable energy sources (iRES), i.e., onshore wind, offshore wind, solar, as a function of the iRES capacity share in a potential 2030 power system of the United Kingdom. Curtailment (blue, left y-axis) and energy surplus (green, right y-axis) data is obtained with the Electricity System Optimisation (ESO) model,^{23,33} which determines optimal electricity dispatch strategy hourly for one year, and does not take transmission constraints into account. Availability data for iRES are taken from ref. 34–36. Curtailment data point for 2016 is derived from National Grid's monthly balancing service reports throughout 2016 referring to total constrained volume including non-iRES fuel types.³⁷

generated power is curtailed; in the night time, however, energy storage is charged with excess power from onshore and offshore wind power. In the sample day on the right hand-side, power availability from iRES is high and again energy storage is utilised. However, as the maximum storage capacity is reached a curtailment of iRES power is economically sensible, avoiding the turn-down/shut-down of nuclear power stations. Overall, we observe higher curtailment levels at night times than during the day. Flexibility of operation is therefore crucial for a process seeking to utilise this surplus electricity. Consequently, several technical/engineering challenges arise. These are discussed in detail in Section 5.

The ESO modelling framework provides the cost-optimal dispatch pattern for electricity generation, but does not

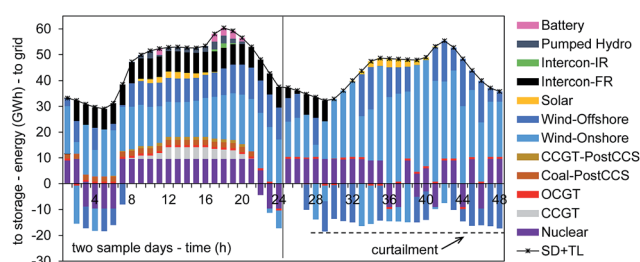


Fig. 3 Optimal dispatch strategy for power generation and storage units in a 2030 UK power system based on the ESO model at an iRES penetration level of 55% of total capacity. The right hand-side sample day operation illustrates an iRES power curtailment event due to excess iRES power generation and the lack of available energy storage capacity. The dashed line represents the maximum storage capacity available which must not be exceeded.

account for lack of grid operator expertise or grid congestion. There is evidence for the UK that constraint payments are still being made to wind farm operators to turn-down their generation, implying that accounting grid congestion and operator expertise are important in reliably predicting the extent to which renewable energy might be curtailed in the future. Curtailed power, therefore, will remain a limited resource for the foreseeable future which should be used in the most efficient way to maximise climate change mitigation.⁴⁰ The present studies focuses on power-to-methanol and power-to-DAC as two options for direct and indirect emission-reductions of the transportation sector. In practice, these routes will further have to compete with grid expansion and other options to utilize electricity (e.g., power-to-heat).⁴⁰

2.2 Non-fossil CO₂

Without final capture and reuse of the CO₂ arising from combustion, the production of CO₂-derived methanol requires the continued extraction of fossil fuels, thus locking us into partial decarbonisation scenarios, quite at odds with the Paris agreement. It is therefore vital that the carbon cycle is closed, and that these emissions are captured and reused. The direct air capture of CO₂ is potentially well-suited for this task. Furthermore, its prospective ease of scale-up (in the case of increased curtailment) owing to its potentially modular nature^{41–43} provides an added advantage.

Direct removal of CO₂ from the air bears similarities to post-combustion capture processes employed by CCS technologies as both are based on chemical absorption. The lower concentrations of CO₂ in air compared to power plant exhaust gases (0.04% and 3–12%, respectively) result in an increased energy cost of capture and render amine solvents unsuitable as they react with the CO₂ in air too slowly.

The majority of academic literature on DAC focuses on hydroxide-based capture, often using sodium or potassium hydroxide as a capture solution. Energetic analyses of proposed DAC technologies specify a wide range of energy costs for capture ranging from 6.7 to 22.7 GJ t_{CO₂}⁻¹, with the upper bound estimates bringing the technical and economic feasibility of the process into question.^{42,44–47}

In this study, the DAC plant assumes a potassium hydroxide (KOH) process, as previously described by Keith⁴⁸ *et al.* and Baciocchi.⁴⁵ It is illustrated in Fig. 4. KOH solution is contacted with ambient air in an absorber where it reacts with the CO₂ in the air to form a carbonate, K₂CO₃. Calcium carbonate fed into

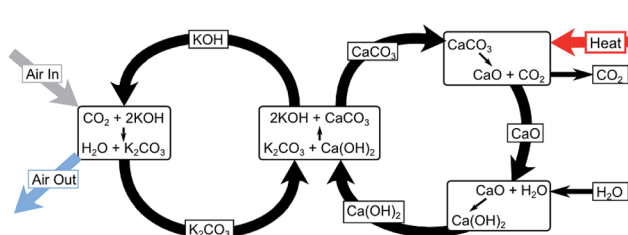


Fig. 4 Chemical reactions involved in the capture of CO₂ directly from the atmosphere using a potassium hydroxide (KOH) solution.⁴²



Table 1 Energy requirements for the lower-bound (carbon engineering) and upper-bound (APS report) direct air capture technologies considered in this work

Technology	Heat requirement (GJ $t_{CO_2}^{-1}$)	Electricity requirement (GJ $t_{CO_2}^{-1}$)	Primary energy requirement (GJ $t_{CO_2}^{-1}$)	Cost (\$ t_{CO_2} avoided $^{-1}$)
Carbon engineering ⁴²	—	5.4	6.7	Not provided
APS report ⁴⁷	6.10	1.78	12.58	610–780

a kiln is then calcined at 900–1000 °C to produce calcium oxide (CaO) which is subsequently hydrated to obtain calcium hydroxide (Ca(OH)₂). CO₂ is produced as a result and is separated for sequestration or CCU purposes. The Ca(OH)₂ produced is reacted with K₂CO₃ to regenerate the capture solution and the cycle is repeated. A high-grade heat input to the kiln is required by the process shown in Fig. 4. The produced CO₂ stream is available at approximately 900 °C – heat is therefore recovered and used to generate electricity which meets the outstanding energy needs of the plant.⁴² This process can be operated using either natural gas or electricity only.⁴² As only curtailed electricity is assumed to be available in this study, an electricity-driven DAC plant is assumed.††

DAC technology is still in the early stages of research and development, and thus evaluating a potential range of energy costs is vital. The lower and upper bound values used in this work were taken from the Carbon Engineering DAC pilot project⁴² and a process design proposed by the American Physical Society, respectively. These processes were selected owing to availability of adequate information for this analysis. Both designs employ hydroxide-based capture as described by Fig. 4. Their heat, electricity and equivalent primary energy requirements are provided in Table 1.

2.3 Green hydrogen

Conventionally, hydrogen is obtained by steam reforming of methane/natural gas. However, to minimise the lifecycle emissions associated with the power-to-fuel process, hydrogen must be obtained from a renewable source. The production of electrolytic hydrogen uses a commercially available technology that can be powered with renewable energy. The theoretical energy demand of the electrolyser is equal to the reaction enthalpy, ΔH . It comprises the changes in Gibbs free energy and entropy, ΔG and $\Delta T.S$, which represent the electricity and heat requirements, respectively, hence increases with temperature. In reality a considerable amount of electrical energy is usually converted into heat energy, due to joule heating of the electrical current which flows through the cell.⁴⁹ ΔG therefore decreases with increasing operating temperature.⁵⁰ In this study, curtailed renewable electricity is the selected energy source, hence lower temperature processes are economically favourable. Consequently, low temperature electrolyzers (LTEs) have been

used in this study. The most common LTEs are alkaline water (AE) and proton-exchange membrane (PEM) electrolyzers. Their operating parameters are provided in Table 2.

The relative simplicity of AEs results in the relatively low capital and operating cost compared to PEMs.⁴⁹ The limited H₂ production rate by PEMs makes AEs doubly advantageous hence they have been used in this study. In alkaline water electrolysis, two electrodes are submerged in a NaOH or KOH solution separated by a membrane, which is only permeable to water and hydroxide. Hydrogen forms at the cathode when electrons are supplied by an external power source. The remaining hydroxide ions migrate through the cell membrane to the anode. A disadvantage of this set-up is the considerable ohmic losses that occur when the electrical current passes through the cell. Furthermore, the membrane limits the maximum current density. Since the separation efficiency of the membrane is not perfect, minor amounts of oxygen will diffuse back into the cathode chamber where it reacts with H₂ to reform water, thereby reducing the process efficiency. Hydrogen diffusion back into the anode chamber occurs especially at lower loads (<40%).⁵² This results in lower system dynamics, which may be a major drawback given the fluctuating nature of the wind energy supplied. However, modern AEs such as the A-range series from NEL hydrogen are optimised to run with wind energy and hence allow flexible, efficient and safe operation across the operating range of 15–100% of the maximum capacity.⁵³

Taking into account the energy dissipated due to system irreversibilities, the molar energy consumption for hydrogen production is 378.9 kJ mol⁻¹ (4.7 kW h N⁻¹ m⁻³ or 189.5 MJ kg⁻¹).⁵⁴ Recent breakthroughs have however improved the efficiency of alkaline water electrolyzers. The NEL A-485 manufactured by NEL hydrogen can produce 99.9% ($\pm 0.1\%$) purity H₂ at 485 N m³ h⁻¹ with a DC power consumption of just 3.8 kW h N⁻¹ m⁻³.⁵³

Table 2 Performance data of conventional alkaline water (AE) and proton-exchange membrane (PEM) electrolyser modules

Specifications	AE ⁵¹	PEM ^{49,51}	Unit
Cell temperature	60–80	50–80	°C
Cell pressure	<30	<30	bar _a
Efficiency (HHV basis)	72%	60%	—
Capacity per module	<2300	<130	—
Specific energy consumption	3.8–7.0	4.5–7.5	kW h N ⁻¹ m ⁻³
Production rate	<760	<10	N m ³ h ⁻¹

†† The process described in the APS report (see Table 1) requires both heat and electricity. For the purpose of this study, an electricity-to-heat conversion efficiency of 45% has been taken into account.



3 Power-to-fuel

3.1 Methanol as a fuel

The methanol economy, as proposed by Asinger⁵⁵ and later by Olah,^{56,57} presents methanol as a ready substitute for transport fuels, suitable energy storage medium and raw material for the production of synthetic hydrocarbons. In internal combustion engines (ICEs), methanol can be used either as a fuel-blend or as a dedicated (100%) fuel, in both spark ignition (SI) and compression ignition (CI) operating modes. While its relative ease of handling at ambient conditions and suitability for ICEs with little modifications are advantageous, clarity on the amount of methanol required to displace fuel for a given purpose is crucial to understanding its potential.

Table 3 highlights the properties of both fuels. While methanol is denser and emits $1.7 \text{ kg}_{\text{CO}_2} \text{ kg}_{\text{fuel}}^{-1}$ less than gasoline, it is inferior if energy density is considered. To determine the amount of methanol needed to displace gasoline, the energy normalisation factor (ENF) and volume normalisation factor (VNF), defined below, are employed:

$$\text{ENF} = \frac{\text{LHV}_{\text{gasoline}}}{\text{LHV}_{\text{methanol}}} = 2.35, \quad (1)$$

$$\text{VNF} = \frac{\rho_{\text{gasoline}}}{\rho_{\text{methanol}}} = 0.95. \quad (2)$$

The equivalence of methanol and gasoline is given by a product of the above, *i.e.* for each litre of gasoline consumed, 2.23 litres of methanol are required to provide the same energy service. Drivers of methanol cars will therefore have to refuel more than twice as often compared to those using gasoline-powered cars. This puts the carbon intensity of using these fuels for transport in perspective—while methanol has significantly lower CO_2 emissions (per kg of fuel) compared to gasoline, its relatively low energy density means that 3.25 g_{CO_2} more are emitted per MJ of energy service provided; a 5% increase relative to the gasoline baseline.

However, there is more to engine performance than simply the energy content of the fuel. Methanol has a relatively high octane number ($\text{RON} = 108.7$), high latent heat of vaporisation (1103 kJ kg^{-1}) and higher oxygen content (50% by mass) compared to gasoline. Blending it with gasoline therefore increases the octane number of the fuel-blend, allowing for higher compression ratios and increased thermal efficiency of

the system. A study investigating the effect of pure methanol over a gasoline engine at different compression ratios reported higher torque output, cylinder output, power output and specific fuel consumption at higher compression ratios.⁵⁸ The high heat of vaporisation leads to a reduction of the temperature of the incoming fuel-air charge, thus increasing the volumetric efficiency and in turn, the power output. The reduced combustion temperatures can lead to simultaneous low soot and NO_x emissions.^{59,60} Reduced soot and smoke emissions also result due to the higher oxygen content. This is particularly important given contemporary focus on the negative human health outcomes associated with the use of gasoline and diesel fuels.

Some issues, however, arise in the use of methanol in internal combustion engines. Its low vapour pressure and high latent heat of vaporisation cause cold start difficulties at low ambient and in-cylinder temperatures, therefore a glow-plug or ignition enhancer is needed.⁶¹ Furthermore, the low lubricity of alcohols, and corrosion susceptibility of metals in alcohols, make fuel additives necessary. Emissions of formaldehyde, acetaldehyde and any unburned methanol are also not sufficiently understood, thus present potential health risks.

In addition, the requirement to carry increased weight will reduce vehicle fuel efficiency.⁶² A 60 L fuel tank can hold 45 kg of gasoline which can provide approximately 2000 MJ (LHV basis). In contrast, 97 kg of methanol are needed to provide the same energy service. The increased weight of methanol needed to substitute a gasoline-provided energy service will therefore result in a fuel efficiency loss. A study into the effects of oxygenates on vehicle performance observed that they led to an efficiency increase of 5% for a car running on 5% methanol and 95% unleaded gasoline (M5).⁶³ Bardaie and Janius, who investigated the effects of alcohol usage in spark-ignition engines, however observed a power loss of 4–5% for a car running on 100% methanol (M100).⁶⁴

Of the energy available from the fuel, only about 25% actually gets applied to moving a car (with a gasoline ICE) or running the accessories, the rest is lost to the exhaust gases, coolant, and friction, as illustrated in Fig. 5.⁶⁵ A reduction in the associated energy losses by ICEs will serve to minimise fuel consumption and improve process efficiency in the future. This conversion ratio has however been assumed for the M100 methanol car in this study (Fig. 6).

On balance, therefore, substituting methanol for gasoline in vehicles will result in a 5% increase in CO_2 emissions per energy service delivered.

Table 3 Some properties of methanol and gasoline as fuels

Fuel	Mass density (kg L^{-1})	Lower heating value ($\text{MJ kg}_{\text{fuel}}^{-1}$)	Carbon density ($\text{kg}_{\text{CO}_2} \text{ kg}_{\text{fuel}}^{-1}$)	Carbon density ($\text{kg}_{\text{CO}_2} \text{ MJ}^{-1}$)
Methanol	0.79	19.7 (ref. 11)	1.375	0.070
Gasoline	0.75	46.4 (ref. 11)	3.088 ^a	0.067

^a Gasoline typically contains a mixture of C4–C12 hydrocarbons. The combustion characteristics of octane (C_8H_{18}) have been used to estimate the carbon density of gasoline.



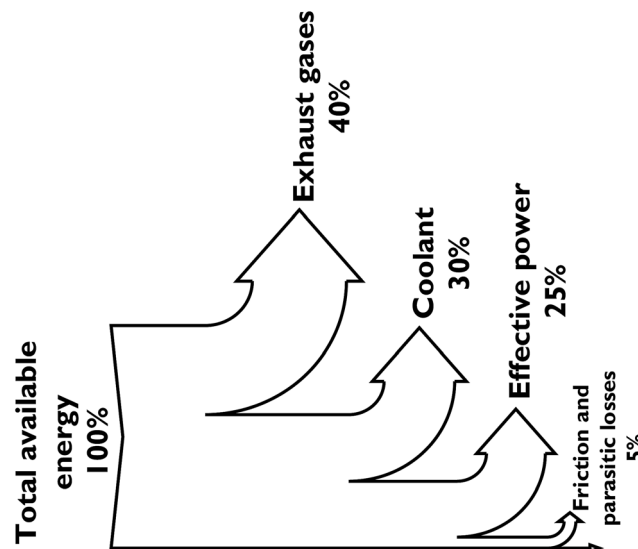


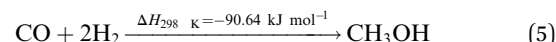
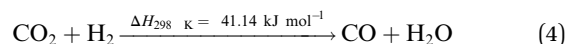
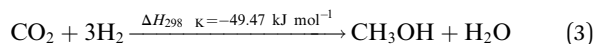
Fig. 5 Sankey diagram showing the energy losses associated with converting chemical energy in gasoline to effective power in an internal combustion engine.

3.2 Methanol production

Methanol synthesis is a commercially viable but mature process. Some reviews covering the development (potential) of this process have been published over the recent years.^{66–68} However, since the process is mature, most research activity relating to methanol revolves around methanol fuel cells,^{69,70} the production of methanol from CO_2 ,^{71–74} as in this study, the reforming of methanol,^{75,76} its use in the synthesis of bio-diesel fuel,^{77,78} its blending properties for fuel blends such as M10,^{79–81} and its transformation in downstream processes into olefins^{82,83} and ultimately, gasoline.^{84,85} China certainly has adopted methanol as a key platform chemical and has become the largest producer – and consumer – of methanol in the world.

Methanol can be produced *via* the catalytic hydrogenation of CO_2 . There are two main reaction pathways – one in which methanol is directly produced according to eqn (3), and

a second in which CO produced *via* the reverse water gas shift (RWGS) reaction is subsequently hydrogenated to produce CH_3OH , according to eqn (4) and (5), respectively.⁷²



An appropriate catalyst needs to be chosen to maximise the CO_2 yield by enhancing the reaction shown in eqn (3) and inhibiting the reaction represented by eqn (4). This would also serve to reduce the operating costs of the process due to reduced recycle. It has been shown that CO_2 and H_2 react directly to form CH_3OH over commercially-available $\text{CuO}/\text{ZnO}/\text{Al}_2\text{O}_3$ catalyst without significant production of CO as an intermediate.⁸⁶

There have been several studies of the production of methanol through catalytic hydrogenation of CO_2 .^{54,87–89} The process designed by Rihko-Struckmann *et al.* makes the same design choices described above, *i.e.* alkaline water electrolyzers and $\text{CuO}/\text{ZnO}/\text{Al}_2\text{O}_3$ catalyst, and has been used as the reference process for this work. Fresh CO_2 and electrolytic hydrogen, which are available at ambient pressure, are compressed to 50 bar before being sent to four adiabatic reactor units in cascade with intercooling. Equilibrium conversion with the defined stoichiometric reactions (eqn (3)–(5)) was assumed. The selected pressure and temperature ranges corresponded to typical industrial conditions for low pressure methanol synthesis.⁵⁴

3.3 Closing the loop

To avoid the partial decarbonisation scenarios discussed earlier and close the CO_2 loop, the CO_2 emissions from the methanol-powered cars must be recaptured and reused. A DAC plant is used to concentrate the atmospheric CO_2 contributed by the cars to high-purity CO_2 feedstock for methanol production by the process described in Section 3.2.

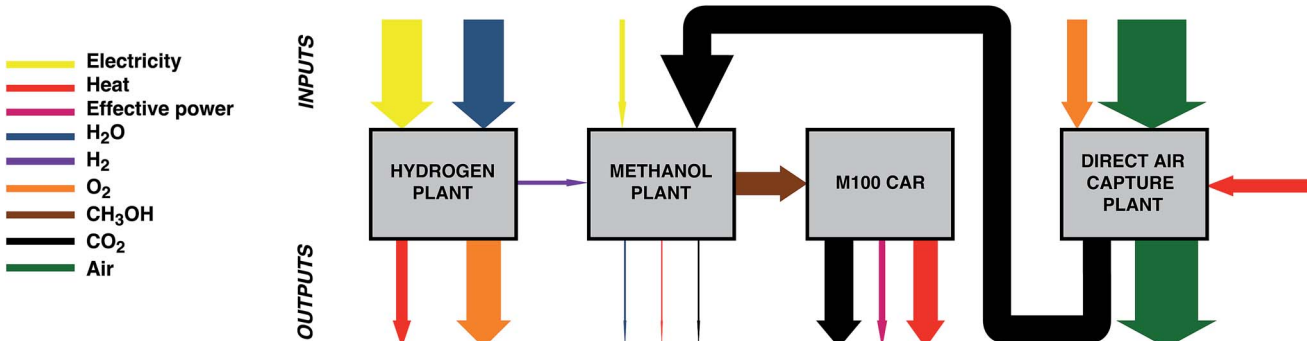


Fig. 6 Simplified representation of the power-to-fuel process showing the mass and energy balances for each unit process. All mass flow rates and energy consumption are drawn to scale relative to the initial water consumption by the electrolyser and energy input to the electrolyser, respectively. Due to the very large flow rates of air required by the direct air capture plant, they have not been drawn to scale for the sake of clarity of the figure.



Table 4 Energy and mass balances for the production of 1 tonne of methanol via the power-to-fuel process

	Hydrogen plant		Methanol plant		Methanol car		Direct air capture plant	
	In	Out	In	Out	In	Out	In	Out
Flow rate (t y⁻¹)								
H ₂ O		1.76			0.08			
H ₂			0.20	0.20				
O ₂			1.57				0.48	
CH ₃ OH					1.00	1.00		
CO ₂				1.44	0.06		1.38	1.38
Air							28.2	26.8
Energy (MWh y⁻¹)								
Electricity	10.31			1.34			2.06	
Heat		3.92			0.25			
Effective power							1.37	
Losses (exhaust, coolant, friction)							4.10	

4 Power-to-DAC

Many studies have concluded that mitigation options such as CCS can only become economically-viable through a combination of policy measures and technological advancement.⁹⁰ CCU, by adding commercial value to CO₂ emissions, is asserted to be able to overcome these challenges. However, the sub-processes involved in the power-to-fuel process described above (electrolysis, methanol production, transport) incur energy losses across the value chain. In addition, a substantial amount of energy is required to recapture the exhaust CO₂ from the atmosphere. Here, the counterfactual of using curtailed wind to directly operate a DAC plant and subsequent storage is considered in order to evaluate the mitigation impact of using renewable energy to operate a DAC process and compare to that of a CCU process.

5 Results and discussion

5.1 The UK as a case study

It is estimated that 1277 GWh of wind power was curtailed in the UK in 2015.⁹¹ This has been used as the basis for the following analysis. The ESO model implies that, unless iRES deployment is increased to over 50% of peak demand, the availability of curtailed renewable electricity is not likely to significantly increase. A near-term ramping of iRES capacity is unlikely owing to the associated grid stability and reliability issues. Additionally, current plans are to expand the UK's interconnection capacity.⁹² This expansion will provide further flexibility to the grid and thus minimise curtailment. Should iRES penetration reach the levels required to see surplus electricity availability, the ESO model suggests that this will be for a few hours per day. This means that the various elements of the power-to-fuel and power-to-DAC processes will be required to operate in a flexible manner, and at low capacity factors, posing additional technical and economic challenges. One such challenge will be for the kiln in the DAC plant. Calcination of CaCO₃ occurs at 900 °C in the kiln. The repeated cooling and heating of the kiln due to intermittent energy

supply will be a source of efficiency loss and may threaten process stability. Therefore, if this course of action is to be pursued, it will be vital to design DAC processes so as to ensure their suitability for this kind of intermittent operation. Furthermore, a plant solely dependent on intermittent energy supply to operate will require labour arrangements that differ from conventional practice.

Table 4 shows the mass and energy balances for the production of a tonne of methanol annually *via* the power-to-fuel process, assuming 1277 GWh y⁻¹ of renewable electricity remain available and the lower-bound energy consumption of 5.4 GJ_e t_{CO₂}⁻¹ for the DAC technology. The arrow widths are scaled to the amount of mass or energy flow required relative to the water and energy input to the electrolyzers, respectively. Due to the dilute nature of CO₂ in air, large volumes of air are needed to capture a substantial amount of CO₂. To recapture the CO₂ emitted by the methanol cars, 17 000 m³ t_{CO₂}⁻¹ and 27 000 m³ t_{CO₂}⁻¹ of air are required by the lower- and upper-bound DAC technologies considered, which have capture efficiencies of 80% and 50%, respectively.

Approximately 12 MWh t_{MeOH}⁻¹ of electricity was required for methanol production alone, with the bulk of the curtailed electricity – 89% – being consumed by the electrolysis plant. An additional 2.1 MWh t_{MeOH}⁻¹ was required to recapture the CO₂ emitted from methanol combustion.

5.2 Mitigation potential

In the UK, gasoline accounts for 33 vol% of transport fuel used in the UK, resulting in the emission of 40 Mt_{CO₂} per year to the atmosphere.⁹³ Here, a mitigation potential (MP) has been defined to quantify the prospects of both power-to-fuel and power-to-DAC processes for avoiding GHG emissions. The MP for the power-to-fuel process has been defined as the percentage of gasoline consumption that can be displaced by the produced methanol (see eqn (6)).

$$MP_{\text{power-to-fuel}} = \frac{\text{methanol produced}}{\text{UK gasoline consumption}} \times ENF \times VNF \quad (6)$$



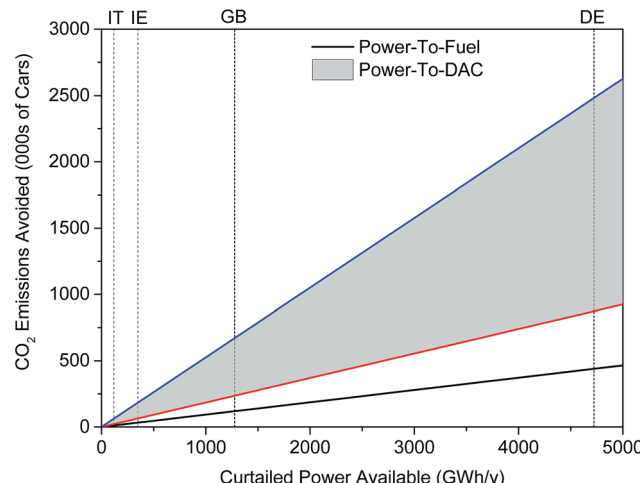


Fig. 7 Mitigation potential of both power-to-fuel and power-to-DAC processes in several EU countries: Italy (IT), Ireland (IE), United Kingdom (GB) and Germany (GE). Curtailment figures were obtained from: IT,⁹¹ IE,⁹⁷ GB⁹¹ and DE.⁹⁸ Note that many countries do not differentiate between constraint and curtailment so these figures may be a sum of both.

while the mitigation potential for the power-to-DAC process is defined as the proportion of gasoline-derived CO₂ emissions that can be avoided if the process is implemented.

$$MP_{\text{power-to-DAC}} = \frac{\text{CO}_2 \text{ emissions avoided by DAC plant}}{\text{UK gasoline-derived emissions}} \quad (7)$$

Thus, 1277 GWh per year of curtailed renewable energy supports the production of approximately 140 million litres of methanol annually. This is enough to displace 62 million litres of gasoline, thereby giving the power-to-fuel process a MP of 0.37%. Power-to-DAC was found to achieve MP values of 2.1% and 0.7% for the lower- and upper-bound energy costs of capture, respectively. Fig. 7 illustrates the mitigation potential of both processes in terms of number of cars for which CO₂ emissions are avoided. A gasoline-powered car is assumed to emit 1.3 t_{CO₂} annually.^{¶¶} Power-to-DAC can avoid the direct CO₂ emissions of 0.24 to 0.67 million cars annually, 2–6 times greater than that achieved by power-to-fuel – 0.12 million cars. While only the emissions from combustion have been taken into account in the above analysis, the same trends have been observed when life cycle analysis (LCA) data is considered.^{40,96}

5.3 Mitigation costs

Methanol production. The economic feasibility of a specific chemical process can be determined by examining related indicators known as economic potentials.⁹⁹ The level 1 economic potential (EP₁) is defined as the ratio of product values (PV) and feedstock costs (FC):

¶¶ Based on average CO₂ emissions and annual mileage of 121.3 g_{CO₂} km⁻¹ (ref. 94) and 6500 miles,⁹⁵ respectively, for gasoline-powered cars in England.

Table 5 Typical prices of chemicals in the methanol synthesis process

Chemicals	Prices, \$ t ⁻¹
Fossil CO ₂ ^a	37–120 (ref. 101)
Non-fossil CO ₂ ^b	450–550 (ref. 47)
Fossil H ₂	1300–2100 (ref. 102 and 103)
Electrolytic H ₂	4200 (ref. 104)
CH ₃ OH	450 (ref. 105)

^a Fossil CO₂ is obtained from a coal plant with post-combustion carbon capture and storage. ^b Non-fossil CO₂ is obtained from a DAC plant.

$$EP_1 = \frac{\sum PV_i}{\sum FC_j} \quad (8)$$

while the level 2 economic potential (EP₂) takes energy costs (EC) into account so that the definition is modified accordingly as below:

$$EP_2 = \frac{\sum PV_i - \sum EC_k}{\sum FC_j} \quad (9)$$

where *i, j, k* denote the products, required feedstock, and the number of process equipment, respectively. If EP₂ > 1, the process is deemed economic feasible, and *vice versa*. For the catalytic hydrogenation of CO₂ to methanol, the selective reaction is as shown in eqn (3), where methanol is assumed to be the only valuable product, and CO₂ and H₂ are the two raw material costs that exert a significant influence on the economic potential. Relevant feed and product prices are listed in Table 5; electricity is assumed to be provided at the same price as that from a combined cycle gas plant at a cost of \$56.4 MWh⁻¹.¹⁰⁰ It has been suggested that surplus electricity will be available at no cost,¹⁵ and that a credit will be available for the mitigation service provided by these processes. However, constraint payments of up to \$225 MWh⁻¹ have been made to UK wind farm operators to curtail their generation, thus, it is expected that they will make this electricity available for utilisation at a price.²⁵ The values of EP₁ and EP₂ were calculated at 0.49 and 0.45, respectively. The EP values being considerably lower than 1 indicate the current economic infeasibility of the power-to-fuel process.

The commercial viability of methanol production was found to be most sensitive to the hydrogen price. This means that as opposed to focusing on developing improved catalysts to enable the cost effective conversion of CO₂ to fuels, it is more important to focus on developing less costly routes to the production of green hydrogen. A study evaluating the economic performance of a plant producing methanol *via* CO₂ hydrogenation with electrolytic hydrogen was found to have a negative margin of \$126 million per year.⁸⁸ This translates to a cost of \$209 t_{CO₂}⁻¹ avoided.^{¶¶} Using this information, a sensitivity analysis was carried out to determine how the profitability of methanol production changes in different feed and product price scenarios. Fig. 8 illustrates the methanol prices needed for the

¶¶ Assuming 2014 exchange rate of 1.3285\$ per €.



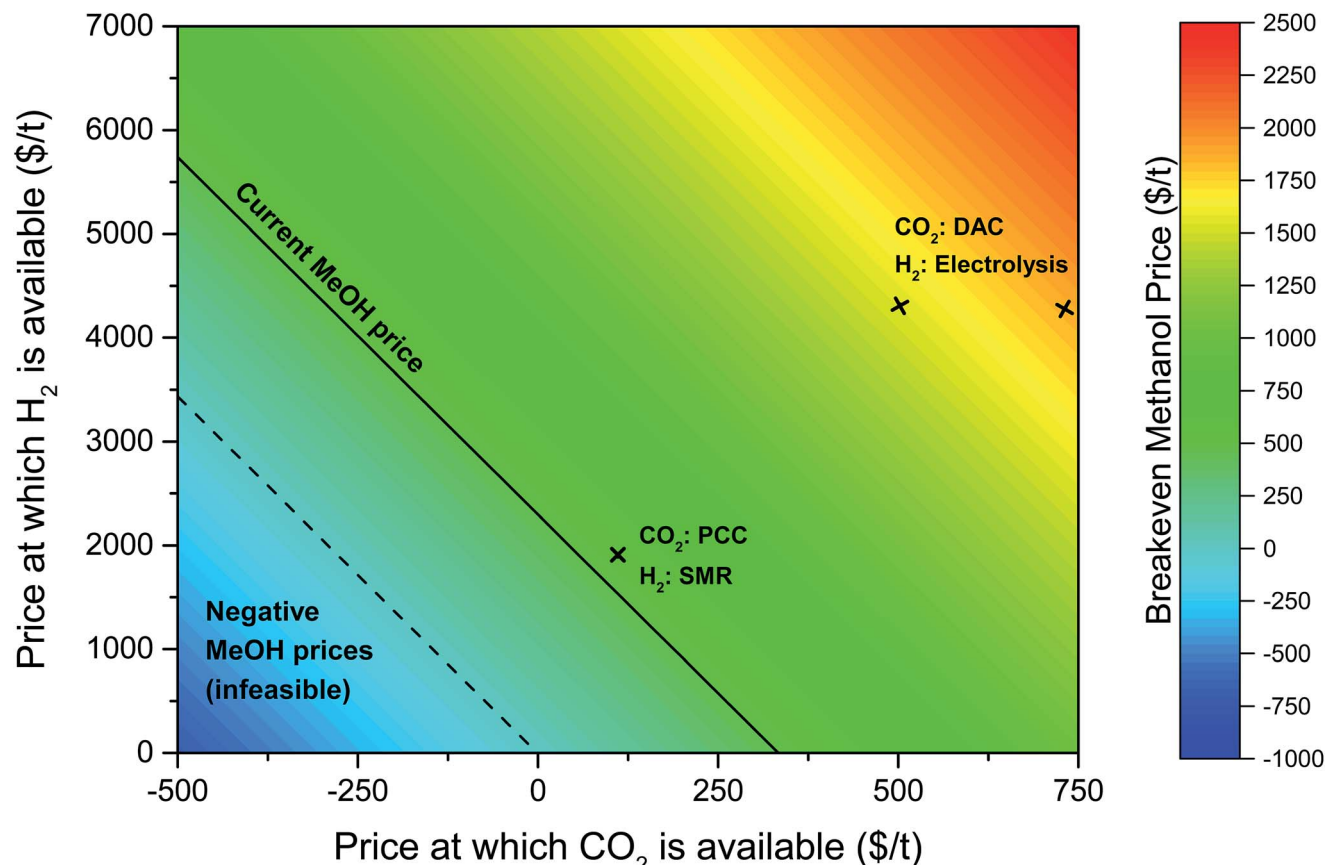


Fig. 8 Contour plot showing the variation in the price of methanol needed with hydrogen and carbon dioxide prices for the methanol production plant to breakeven after 20 years. The solid black line indicates the current price of methanol ($\$450 \text{ t}^{-1}$) and the dashed black line indicates zero methanol price, *i.e.* the point below which the breakeven price of methanol is negative. The breakeven methanol price when CO_2 is sourced from a coal plant with post-combustion capture (PCC)¹⁰⁶ and hydrogen from steam methane reforming (SMR) of natural gas¹⁰² is also highlighted. The breakeven methanol prices for the power-to-fuel process considered in this study (using CO_2 via direct air capture (DAC) and electrolytic hydrogen) are also shown above. Note that a range of prices for fossil-derived H_2 and CO_2 is available in the literature (see Table 5), which will slightly alter the breakeven price of methanol.

plant to break-even after its assumed 20 year lifetime. It is important to note that intermittent nature of energy supply, which will increase the capital costs of the methanol production plant, was not considered in the cited study.

At today's hydrogen and carbon dioxide prices (see Table 5), methanol price must more than double to $\$960 \text{ t}_{\text{MeOH}}^{-1}$ for the plant to break even; if carbon dioxide and methanol prices stayed constant, then the hydrogen price would need to reduce by a factor of 2.6 to $\$1635 \text{ t}_{\text{H}_2}^{-1}$; if hydrogen and methanol prices stayed constant, a credit of $\$283 \text{ t}_{\text{CO}_2 \text{ avoided}}^{-1}$ would need to be provided. Annotated in Fig. 8 is the methanol price if CO_2 and H_2 were sourced from cheaper alternative processes, at costs equivalent to CO_2 from a post-combustion capture (PCC) from a power plant and H_2 from the steam reforming of methane (SMR). This would still require a methanol price of $\$523 \text{ t}_{\text{MeOH}}^{-1}$, 16% higher than current prices. It is important to note that both of these alternatives involve fossil fuel use, hence are contrary to our objective of maximising the mitigation potential of renewable electricity.

Direct air capture. The 2011 APS report presented a techno-economic assessment for a proposed DAC plant capturing 1 Mt_{CO_2} per year. The cost of capture was evaluated to be $\$430\text{--}550 \text{ t}_{\text{CO}_2}^{-1}$.⁴⁷ The cost per tonne of CO_2 avoided, C_{avoided} , can be evaluated using eqn (10) below.

$$C_{\text{avoided}} = \frac{C_{\text{capture}}}{1 - c_Q Q - c_W W} \quad (10)$$

where c_Q and c_W are the carbon intensities of the heat and power supply ($\text{t}_{\text{CO}_2} \text{ GJ}^{-1}$), respectively, and Q and W are the external heat and work inputs ($\text{GJ t}_{\text{CO}_2}^{-1}$), respectively. All heat and work requirements are met using curtailed renewable electricity so c_W and c_Q are assumed to be zero. Should heat requirements be met using natural gas, a c_Q of $0.02 \text{ GJ t}_{\text{CO}_2}^{-1}$ must be taken into account.*** Using the energy requirements provided in Table 1, the DAC plant is estimated to incur costs of $430\text{--}660 \text{ \$ t}_{\text{CO}_2}^{-1}$ avoided (see Fig. 9).

*** Properties of methane have been assumed for natural gas (HHV of 55.5 MJ kg^{-1} and complete combustion producing $2.75 \text{ kg}_{\text{CO}_2} \text{ kg}_{\text{NG}}^{-1}$).

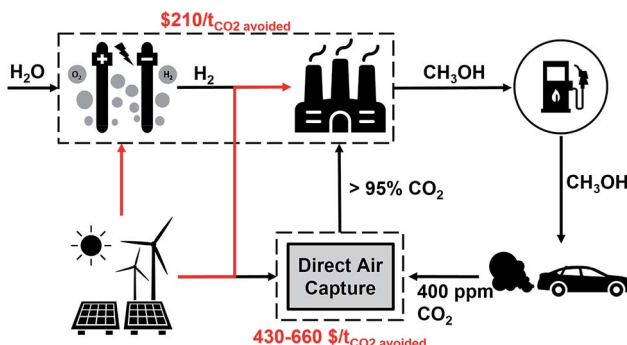


Fig. 9 Costs per tonne of CO_2 avoided for the unit processes involved in the power-to-fuel and power-to-DAC processes. Numbers in red indicate a financial cost.

5.4 Process improvements

Co-location of plants. The lower- and upper-bound DAC technologies considered in this work, when operated using natural gas, include an air separation unit (ASU) to provide oxygen (O_2) for the oxy-fired natural gas combustion. Burning the natural gas in air would mean a substantial amount of nitrogen will be present, along with CO_2 , in the captured exhaust thus requiring a further post-combustion separation to obtain pure CO_2 . The electrolysis plant that provides hydrogen

feed into the reactor produces $172 \text{ kt}_{\text{O}_2}$ annually as a by-product, which has thus far been assumed to be vented to the atmosphere. The possibility of using the electrolyser as a source of oxygen for the DAC plant in power-to-fuel was considered as this would offset some of the energy costs (from the plant's air separation unit). The DAC plant consumes $72 \text{ kt}_{\text{O}_2} \text{ y}^{-1}$, therefore using O_2 from the electrolyser eliminates the need for an ASU in the DAC facility. Fig. 10 illustrates the process flow diagram for the power-to-fuel process if the electrolysis and DAC plants are co-located. The dashed black line represents the O_2 produced by the electrolyzers being fed into the DAC plant for oxy-combustion with natural gas. The ASU no longer required is shown in subtle detail (Fig. 11).

Conventional cryogenic air separation consumes $245 \text{ kW h t}_{\text{O}_2}^{-1}$ produced.¹⁰⁷ Co-location of the electrolysis and DAC plants could therefore provide energy savings in the range $17\text{--}34 \text{ GWh y}^{-1}$ for the lower and upper bound DAC technologies considered, respectively, equivalent to 6% of the annual primary energy consumption by the DAC plants. ASU costs of $\$10\text{--}100 \text{ t}_{\text{O}_2}^{-1}$ have been cited in the literature¹⁰⁸ so co-locating the plants can drive down mitigation costs by $\$5\text{--}48 \text{ t}_{\text{CO}_2}^{-1}$.

Direct air capture. The heat required to calcine CaCO_3 is required to be at a temperature greater than $\sim 1223 \text{ K}$, practically necessitating the combustion of a fuel (and this must be done using an oxy-fired system to produce a pure stream of CO_2). Usual practice in the calcium looping cycle for CO_2

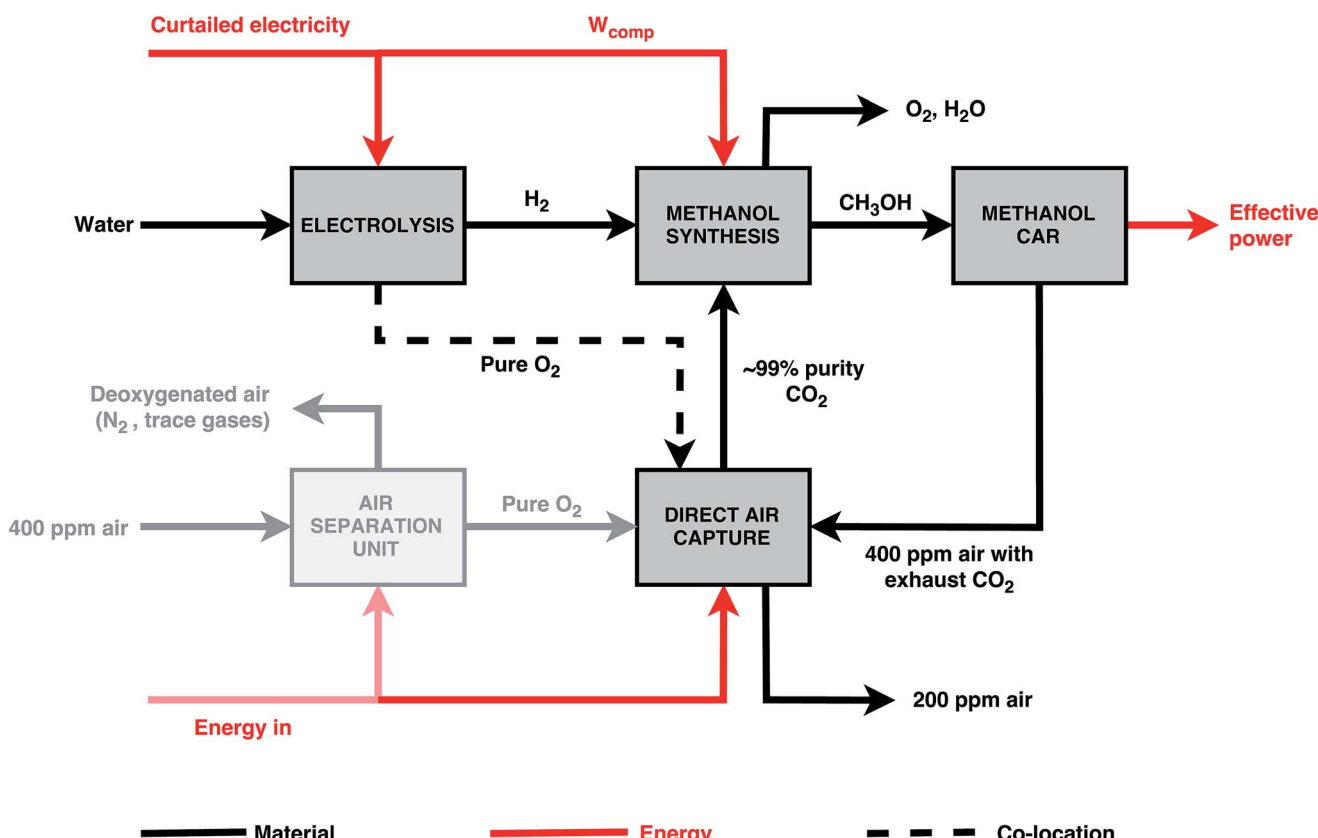
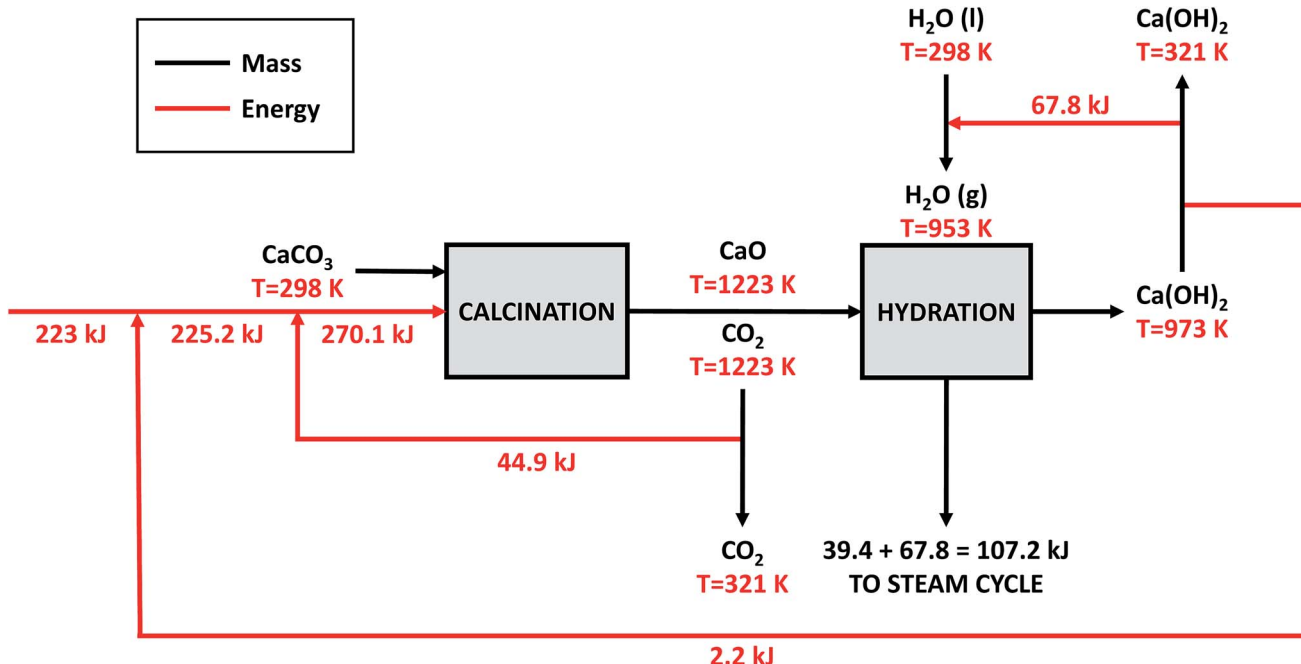


Fig. 10 Process flow diagram for the power-to-fuel process showing the O_2 source if electrolysis and DAC plants are co-located. Dashed black line represents the O_2 produced by the electrolyzers being fed into the DAC plant.



Integrate with steam cycle 223 kJ of heat required, 107.2 kJ of electricity produced

Fig. 11 Proposed heat integration for the direct air capture process proposed in the 2011 APS report.

capture from a power station would be to integrate a steam cycle at around 973 K . This very significantly enhances the process efficiency. However, in the cycle proposed for CO_2 capture from the air, the exothermic CO_2 capture stage occurs at ambient temperature, effectively slightly increasing the air temperature, but wasting the opportunity to integrate heat, effectively throwing away 100% of the high grade heat. The opportunity exists to potentially operate a steam cycle to reclaim some of the hydration heat, but this requires pressurisation of the hydrator – see Appendix 1 for details. Heat integration could potentially reduce the primary energy demand of the upper-bound DAC plant to $8.79\text{ GJ t}_{\text{CO}_2}^{-1}$ captured. This could save 157 TJ y^{-1} , or approximately 30% of the natural gas requirement of the plant. The reconversion efficiency of the power-to-fuel process is therefore increased from 33.3% to 36.5% (η is increased from 8.3% to 9.1% if power-to-mobility is considered).

Commercial pursuit of DAC technology has largely focused on modular units that allow for ease of scale-up.^{41–43} This, potentially, creates scope for cost reduction through mass production. As DAC technology is common to both the power-to-fuel and the power-to-DAC processes discussed in this study, their relative costs will be independent of the actual cost of DAC.

6 Conclusions

CCU is often proposed as a means to improve the economic viability of CO_2 mitigation. To reduce the associated life-cycle emissions of CO_2 -based fuels compared to fossil fuels, the material and energy inputs typically need to be derived from

renewable sources. CCU processes often aim to use curtailed renewable electricity. As the UK electricity system transforms to meet its decarbonisation target, this study finds that material levels of curtailment are unlikely at iRES penetration levels of <50%, which are unlikely before 2035. Furthermore, whilst it is evident that instances of surplus renewable energy have existed in different regions, measures being pursued, including the expansion of regional transmission networks, will serve to keep curtailment below contemporary levels. The curtailed power is unlikely to be available at zero cost, as evidenced by the constraint payments being made to UK wind farms to curtail their generation. Therefore, arguments basing CCU process operations only on the use of curtailed iRES are not likely.

However, where curtailed renewable energy does exist, direct removal of CO_2 from the atmosphere *via* direct air capture (DAC) can mitigate 2–6 times more CO_2 than converting CO_2 into methanol, per unit of available energy. On the basis of 1277 GWh y^{-1} electricity availability, DAC can avoid $0.7\text{--}2.1\%$ of the UK's 2016 gasoline-derived emissions at a cost of $\$430\text{--}660\text{ t}_{\text{CO}_2\text{ avoided}}^{-1}$. Using this electricity for methanol production and subsequent recycling of CO_2 , however, can avoid 0.37% of gasoline-derived emissions at a cost of $\$640\text{--}870\text{ t}_{\text{CO}_2\text{ avoided}}^{-1}$. The additional costs incurred by methanol production are largely due to the cost of H_2 feedstock which significantly outweigh the revenue from methanol sale. We find that in terms of mitigation potential and costs, power-to-DAC is better than power-to-fuel in all scenarios. Furthermore, low-pressure methanol synthesis is a commercially-viable and mature process.^{66–68,109} DAC technology, however, is still a novel technology with current RD&D efforts geared towards developing



modular systems, providing promise for cost reduction and scalability. Both power-to-fuel and power-to-DAC processes would benefit from better DAC systems.

Appendix 2 discusses the opportunities for advancement in methanol synthesis technology and catalysts. It was found that even if the catalyst is improved to further facilitate methanol production, the costs of non-fossil CO₂ and electrolytic hydrogen must reduce significantly for the power-to-fuel process to be economically feasible.

A core conclusion of this study is that using surplus renewable energy to capture CO₂ directly from the atmosphere *via* DAC is a superior option, both from an environmental and an economic point of view, to using it to produce methanol for use as a gasoline substitute. Thus, more CO₂ emissions would be avoided if fossil fuels are further burned and renewable energy is used for DAC than by converting the captured CO₂ into fuels.

This study has focused on the maximum climate change mitigation that is achievable for a given supply of surplus electricity. Should curtailed electricity be used, the electrolysis, methanol and DAC plants must be designed for intermittent operation, *i.e.* at low load factors. Consequently, the labour arrangements will differ from conventional practice in chemical plants. This could have significant implications on costs. The analysis in Fig. 8 illustrates the effects of increased CO₂ and H₂ prices on the breakeven price of methanol, which determines the financial viability of the process. Our analysis neglected the effects of intermittency and thus presents an optimistic scenario. To quantify the impact of intermittent operation on capital and operating costs, detailed design of the individual processes is needed, which is beyond the scope of this current study. Since intermittency would affect both power-to-methanol and power-to-DAC plant, we believe that main findings of the comparison of both routes would still remain valid given a more detailed analysis.

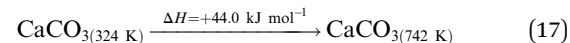
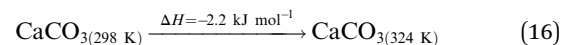
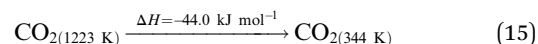
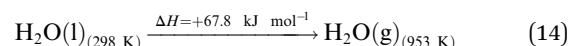
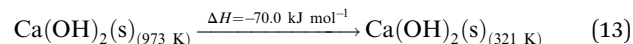
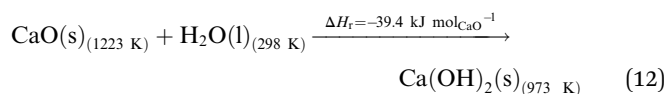
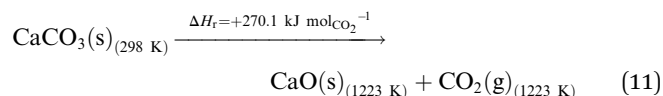
7 Implications for policymakers

There are two primary conclusions to this study. First, in any well-designed and professionally operated electricity system, the spectre of significant quantities of curtailed renewable energy is unlikely to appear in the medium to long term. For this reason, arguments to support initiatives aimed at utilising this curtailed renewable energy should be viewed with caution. Second, in order to avoid lock-in to partial decarbonisation scenarios, any fossil carbon which is extracted from the geosphere must be promptly returned to the geosphere. In net-zero and net-negative emission scenarios, processes which seek to convert carbon to short-lived products – essentially all CO₂ utilisation options aside from mineral carbonation – will need to be coupled with direct air capture or use biomass feedstock to recapture the CO₂ arising from these processes. This has the consequence that on a technical, economic and climate change mitigation basis, direct air capture and subsequent CO₂ storage would appear to offer superior value than the conversion of CO₂. Still, policymakers and societies might opt for the less efficient route *via* conversion of CO₂ due to public acceptance, or increased energy security. The present study quantifies the

corresponding significant increase in cost and loss in mitigation efficiency which have to be taken into account.

Appendix 1

The DAC design presented in the APS report has simply considered the energy requirement for heating CaCO₃ from 298 K to around 1223 K, followed by calcination, to achieve the figure of 6.1 GJ t_{CO₂} captured⁻¹, with an appropriate kiln efficiency then assumed on top of this figure (to yield a total of 6.1/η_{kiln} = 8.13 GJ t_{CO₂}⁻¹ primary energy requirement). Considering the flowsheet in Fig. 1 carefully, there is the possibility of reclaiming some heat from the exothermic hydration reaction described in eqn (12). This could be either used to preheat the CaCO₃ entering the kiln or alternatively used to raise steam to offset some of the on-site electricity costs. Prior to heat integration, the main reactions are eqn (11) and (12), calcination and hydration (including relevant temperature changes). To obtain heat at a sufficiently high temperature for either effective preheating or electricity generation, the hydration reactor would have to be pressurized. Here, it has been assumed that the pressure is maintained at 16.3 bar_a, corresponding to the equilibrium pressure for the reaction between CaO and H₂O at 973 K. CaO(s) is presumed to be produced at 1223 K, and H₂O(l) is available at ambient temperature, 298 K. All heat exchangers have been assumed to require 20 K temperature difference.



High temperature calcination (eqn (11)) comprises majority of the heat requirement of the system. Heat is available at 973 K *via* reaction 12, and from the cooling of Ca(OH)₂ from reaction temperature to near ambient temperature, eqn (13). The heat liberated in reaction (14) can be used to vapourise and preheat water *via* eqn (16), with the potential for a small preheat of CaCO₃ with any remaining heat from eqn (16). This would effectively increase the energy available to produce electricity *via* reaction (12), and very slightly decrease the heat requirement for reaction (11). There is of

course heat available from cooling down the hot CO_2 , which can be used to further raise the temperature of the CaCO_3 which was preheated under eqn (16) *via* eqn (17). Failure to integrate with a steam cycle severely limits the heat integration possibilities of the process.

The scheme above yields a heat requirement of 223.9 kJ and yields 107.2 kJ of energy to be taken out in a steam cycle. This is equivalent to $5.08 \text{ GJ}_{\text{th}} \text{ t}_{\text{CO}_2}^{-1}$ ($6.78 \text{ GJ} \text{ t}_{\text{CO}_2}^{-1}$ of primary energy after taking into account kiln efficiency) and with electricity assumed to be produced from the steam cycle with an efficiency of 40%, yielding $0.97 \text{ GJ}_{\text{e}} \text{ t}_{\text{CO}_2}^{-1}$, with a net import $0.81 \text{ GJ}_{\text{e}} \text{ t}_{\text{CO}_2}^{-1}$, requiring $2.01 \text{ GJ} \text{ t}_{\text{CO}_2}^{-1}$ of natural gas to produce. Overall, this yields a net heat requirement of $8.79 \text{ GJ} \text{ t}_{\text{CO}_2}^{-1}$. The scheme described here is, as far as we can see, the most heat integrated method possible (and does not take into account capital costs, which may well be very large). It is not proposed to consider heat transfer within the KOH part of the process, since heat recovery from the aqueous solutions will be challenging, the heat of reaction for the CO_2 transfer from potassium to carbonate is small, and the large air flows will continually cool the circulating solution to ambient temperature.

If the primary energy requirement of the DAC processes presented in the APS report⁴⁷ (upper-bound DAC plant) is reduced to $8.79 \text{ GJ} \text{ t}_{\text{CO}_2 \text{ captured}}^{-1}$ *via* the heat integration presented above, $157 \text{ TJ} \text{ y}^{-1}$ could be saved. This is equivalent to 30.2% of the natural gas requirement of the plant. The reconversion efficiency of the power-to-fuel process is therefore increased from 33.3% to 36.5% (η is increased from 8.3% to 9.1% if power-to-mobility is considered).

Appendix 2

Research priorities

Methanol synthesis technology opportunities. Typically, methanol synthesis is carried out in the gas phase in fixed-bed reactors (either near isothermally – Lurgi, or adiabatically – ICI, Synetix or, following the maximum rate curve – Mitsubishi). Since the overall methanol synthesis reaction (from CO) is highly exothermic ($\Delta H = -90.84 \text{ kJ mol}^{-1}$) it is very difficult to control the temperature in these reactors and avoid consequential catalyst deactivation. To overcome this limitation liquid-phase slurry bubble reactor systems similar to those employed in Fischer-Tropsch synthesis (also a very exothermic reaction) could be employed.¹¹⁰ Liquid-phase methanol synthesis would also allow for facile catalyst exchange. Such a system was first demonstrated by Air Products and the US Department of Energy (LPMEOHTM). This would require the development of highly active colloidal catalyst systems, which is an ongoing effort.^{111,112} Another liquid-phase system proposed and developed by Brookhaven National Laboratory and AMOCO demonstrated the application of transition metal-based homogeneous catalysts ($\text{Ni}(\text{CO})_4$ -based) – this has significant safety implications in terms of catalyst handling. In principle, methanol synthesis at low temperatures may be desirable from an equilibrium point of view, however a sufficiently large thermal gradient is required in a commercial process to efficiently remove the heat of reaction and utilise this heat elsewhere in

the plant, thus limiting the desirable operating temperature of methanol synthesis to above, say, 170 °C. One interesting opportunity would be the operation at very high pressure in order to afford virtually complete conversion and thus remove the need for costly recycle.¹¹³

Methanol synthesis catalytic opportunities. Since every chemical process is governed by the performance of the reactor (up- and downstream processing) and, for a catalytic system, the performance of the catalyst within, there are still plenty of opportunities to improve methanol synthesis. A highly-active research field in this context is the hydrogenation of CO_2 instead of syngas to yield methanol. Many (catalytic) approaches are being followed and a number of recent reviews summarise the current state of the art.^{71,72,114} The fundamental issue is the cost of capturing CO_2 and producing renewable hydrogen *versus* that of simply generating syngas. Many techno-economic analyses have been performed including several life-cycle assessment studies showing that renewable energy is required to obtain CO_2 savings compared to fossil methanol.^{88,96} Most analyses also do not project properly how the cost of methanol would develop and how the logistics would be solved, let alone the issue of sourcing renewable reducing equivalents (hydrogen or electrons).^{114,115}

The catalytic holy grail of methanol synthesis is, of course, the direct partial oxidation of methane to methanol.¹¹⁶ Research has covered high-temperature systems, which are unlikely to become commercially viable as it is difficult to exert sufficient control in radical reactions to afford the required selectivity at appreciable conversion.^{117,118} Low temperature synthesis has been demonstrated with highly acidic systems that can stabilise methyl groups.¹¹⁹ Industrially this would require costly materials to deal with the acid nature of the process. Routinely, biological systems perform this reaction at high turnover frequencies and room temperature. The enzyme (catalyst) facilitating this action is methanol mono-oxygenase (MMA).¹²⁰ Inorganic equivalents bases on Cu and Fe exchanged zeolites have shown significant activity and selectivity.^{121,122} However, selectivity and yields need to be improved significantly to give this approach industrial relevance.

Conflicts of interest

There are no conflicts to declare.

Acknowledgements

The authors thank the “Science and Solutions for a Changing Planet Doctoral Training Programme” (SSCP DTP) by the Natural Environment Research Council (NERC), the Department of Chemical Engineering at Imperial College London, the IEA Greenhouse Gas R&D Programme (IEAGHG) and the MESMERISE-CCS project under grant EP/M001369/1 from the Engineering and Physical Sciences Research Council (EPSRC) for the funding of PhD scholarships and support of this project. The authors are grateful to Dr J. Yao for his help in checking the calculations presented in Appendix 1. André Bardow acknowledges that part of this work was supported by the Cluster of



Excellence "Tailor-Made Fuels from Biomass", which is funded under contract EXC 236 by the Excellence Initiative by the German federal and state governments to promote science and research at German universities.

References

- 1 IPCC, *Climate Change 2014: Mitigation of Climate Change*, Cambridge University Press, Cambridge, United Kingdom, 2014.
- 2 G. Lomax, T. M. Lenton, A. Adeosun and M. Workman, *Nat. Clim. Change*, 2015, **5**, 498–500.
- 3 E. Kriegler, O. Edenhofer, L. Reuster, G. Luderer and D. Klein, *Clim. Change*, 2013, **118**, 45–57.
- 4 P. Smith, S. J. Davis, F. Creutzig, S. Fuss, J. Minx, B. Gabrielle, E. Kato, R. B. Jackson, A. Cowie, E. Kriegler, D. P. van Vuuren, J. Rogelj, P. Ciais, J. Milne, J. G. Canadell, D. McCollum, G. Peters, R. Andrew, V. Krey, G. Shrestha, P. Friedlingstein, T. Gasser, A. Grübler, W. K. Heidug, M. Jonas, C. D. Jones, F. Kraxner, E. Littleton, J. Lowe, J. R. Moreira, N. Nakicenovic, M. Obersteiner, A. Patwardhan, M. Rogner, E. Rubin, A. Sharifi, A. Torvanger, Y. Yamagata, J. Edmonds and C. Yongsung, *Nat. Clim. Change*, 2015, **6**, 42–50.
- 5 M. Fajardy and N. Mac Dowell, *Energy Environ. Sci.*, 2017, **10**, 1389–1426.
- 6 P. Psarras, H. Krutka, M. Fajardy, Z. Zhang, S. Liguori, N. M. Dowell and J. Wilcox, *Wiley Interdiscip. Rev.: Energy Environ.*, 2017, **6**, e253.
- 7 I. Dimitriou, P. Garcia-Gutierrez, R. H. Elder, R. M. Cuellar-Franca, A. Azapagic and R. W. K. Allen, *Energy Environ. Sci.*, 2015, **8**, 1775–1789.
- 8 M. E. Boot-Handford, J. C. Abanades, E. J. Anthony, M. J. Blunt, S. Brandani, N. Mac Dowell, J. R. Fernandez, M.-C. Ferrari, R. Gross, J. P. Hallett, R. S. Haszeldine, P. Heptonstall, A. Lyngfelt, Z. Makuch, E. Mangano, R. T. J. Porter, M. Pourkashanian, G. T. Rochelle, N. Shah, J. G. Yao and P. S. Fennell, *Energy Environ. Sci.*, 2014, **7**, 130–189.
- 9 J. Klankermayer, S. Wesselbaum, K. Beydoun and W. Leitner, *Angew. Chem., Int. Ed.*, 2016, **55**, 7296–7343.
- 10 P. Markewitz, W. Kuckshinrichs, W. Leitner, J. Linssen, P. Zapp, R. Bongartz, A. Schreiber and T. E. Muller, *Energy Environ. Sci.*, 2012, **5**, 7281–7305.
- 11 N. Mac Dowell, P. S. Fennell, N. Shah and G. C. Maitland, *Nat. Clim. Change*, 2017, 243–249.
- 12 J. G. Olivier, G. Janssens-Maenhout, M. Muntean and J. A. Peters, *Trends in global CO₂ emissions: 2015 Report*, PBL Netherlands Environmental Assessment Agency, 2015.
- 13 N. von der Assen and A. Bardow, *Green Chem.*, 2014, **16**, 3272–3280.
- 14 U.S. Energy Information Administration, *Short-Term Energy Outlook (STEO)*, 2017.
- 15 G. Wilson, M. Trusler, J. Yao, J.-S. M. Lee, R. Graham, N. Mac Dowell, R. Cuellar-Franca, G. Dowson, P. Fennell, P. Styring, J. Gibbins, M. Mazzotti, S. Brandani, C. Muller and R. Hubble, *Faraday Discuss.*, 2016, **192**, 561–579.
- 16 J. Petrinrin and M. Shaaban, *Renewable Sustainable Energy Rev.*, 2016, **65**, 770–783.
- 17 C. F. Heuberger, I. Staffell, N. Shah and N. Mac Dowell, *Energy Environ. Sci.*, 2016, **9**, 2497–2510.
- 18 L. Bird, D. Lew, M. Milligan, E. M. Carlini, A. Estanquero, D. Flynn, E. Gómez-Lázaro, H. Holtinnen, N. Menemenlis, A. Orths, P. B. Eriksen, J. C. Smith, L. Soder, P. Sorensen, A. Altiparmakis, Y. Yasuda and J. Miller, *Renewable Sustainable Energy Rev.*, 2016, **65**, 577–586.
- 19 Y. Scholz, H. C. Gils and R. Pietzcker, *Energy Econ.*, 2016, **64**, 568–582.
- 20 National Grid, *Monthly Balancing Services Summary 2014/15*, 2015.
- 21 Y. Yasuda, L. Bird, E. M. Carlini, A. Estanquero, D. Flynn, A. Forcione, E. Gómez-Lázaro, P. Higgins, H. Holtinnen, D. Lew, S. Martin-Martinez, J. McCann, N. Menemenlis and J. C. Smith, *Proceedings of WIW2015 Workshop*, 2015.
- 22 P. Heptonstall, R. Gross and F. Steiner, *The costs and impacts of intermittency – 2016 update*, 2017.
- 23 C. F. Heuberger, I. Staffell, N. Shah and N. M. Dowell, *Comput. Chem. Eng.*, 2017, **107**, 247–256.
- 24 A. Energiewende, *Die Energiewende im Stromsektor: Stand der Dinge 2016. Rückblick auf die wesentlichen Entwicklungen sowie Ausblick auf 2017*, 2016.
- 25 Renewable Energy Foundation (REF), *Wind Farm Constraint Payments over Easter 2016*, 2016.
- 26 European Wind Energy Association (EWEA), *Transmission system operation with a large penetration of wind and other renewable electricity sources in electricity networks using innovative tools and integrated energy solutions (TWENTIES): Final report*, 2013.
- 27 E. V. Mc Garrigle, J. P. Deane and P. G. Leahy, *Renewable Energy*, 2013, **55**, 544–553.
- 28 R. Golden and B. Paulos, *Electr. J.*, 2015, **28**, 36–50.
- 29 M. Rothleder, *Renewable Integration*, California Energy Commission IEPR Workshop, 2017.
- 30 N. Haga, V. Kortela and A. Ahnger, *Reducing Wind Power Curtailment in China*, WÄRTSILÄ White Paper, 2016.
- 31 Ea Energy Analyses, *The Danish Experience with Integrating Variable Renewable Energy, Study on behalf of Agora Energiewende*, 2015.
- 32 Department of Energy & Climate Change, *Updated energy and emissions projections 2015*, 2015.
- 33 C. F. Heuberger, E. Rubin, I. Staffell, N. Shah and N. M. Dowell, *Appl. Energy*, 2017, **204**, 831–845.
- 34 S. Pfenninger and I. Staffell, *Renewables.ninja*, 2016, <https://beta.renewables.ninja/>, accessed: 2017-07-05.
- 35 I. Staffell and S. Pfenninger, *Energy*, 2016, **114**, 1224–1239.
- 36 S. Pfenninger and I. Staffell, *Energy*, 2016, **114**, 1251–1265.
- 37 National Grid, *Monthly Balancing Services Summary 2016*, 2016.
- 38 UK Department of Business, Energy and Industrial Strategy (BEIS), *Updated Energy and Emissions Projections 2016*, 2017.
- 39 Committee on Climate Change, *Sectoral scenarios for the Fifth Carbon Budget*, 2015.



40 A. Sternberg and A. Bardow, *Energy Environ. Sci.*, 2015, **8**, 389–400.

41 Climeworks AG, *Climeworks CO₂ Capture Demonstrator*, 2016.

42 Carbon Engineering Ltd, *Our Technology*, 2015.

43 Global Thermostat Ltd, *About Us: A Unique Capture Process*, 2010.

44 M. Ranjan and H. J. Herzog, *Energy Procedia*, 2011, **4**, 2869–2876.

45 R. Baciocchi, G. Storti and M. Mazzotti, *Chem. Eng. Process.*, 2006, **45**, 1047–1058.

46 K. S. Lackner, *Sci. Am.*, 2010, **302**, 66–71.

47 R. Socolow, M. Desmond, R. Aines, J. Blackstock, O. Bolland, T. Kaarsberg, N. Lewis, M. Mazzotti, A. Pfeffer, K. Sawyer, J. Siirala, B. Smit and J. Wilcox, *Direct Air Capture of CO₂ with Chemicals. A Technology Assessment for the APS Panel on Public Affairs*, 2011.

48 D. W. Keith, M. Ha-Duong and J. K. Stolaroff, *Clim. Change*, 2006, **74**, 17–45.

49 M. Carmo, D. L. Fritz, J. Mergel and D. Stolten, *Int. J. Hydrogen Energy*, 2013, **38**, 4901–4934.

50 M. Laguna-Bercero, *J. Power Sources*, 2012, **203**, 4–16.

51 J. G. Tom Smolinka and M. Günther, *Stand und Entwicklungspotenzial der Wasserelektrolyse zur Herstellung von Wasserstoff aus regenerativen Energien*, 2011.

52 V. Schröder, B. Emonts, H. Janßen and H.-P. Schulze, *Chem. Eng. Technol.*, 2004, **27**, 847–851.

53 NEL Hydrogen, *Efficient Electrolysers for Hydrogen Production*, https://wpstatic.idium.no/www.nel-hydrogen.com/2015/03/Efficient_Electrolysers_for_Hydrogen_Production.pdf, 2016.

54 L. K. Rihko-Struckmann, A. Peschel, R. Hanke-Rauschenbach and K. Sundmacher, *Ind. Eng. Chem. Res.*, 2010, **49**, 11073–11078.

55 F. Asinger, in *Methanol — Chemie- und Energierohstoff*, Springer, Berlin Heidelberg, 1986, pp. 1–9.

56 G. A. Olah, *Angew. Chem., Int. Ed.*, 2005, **44**, 2636–2639.

57 G. A. Olah, A. Goeppert and G. K. S. Prakash, *J. Org. Chem.*, 2009, **74**, 487–498.

58 M. B. Çelik, B. Özدalyan and F. Alkan, *Fuel*, 2011, **90**, 1591–1598.

59 M. Eyidogan, A. N. Ozsezen, M. Canakci and A. Turkcan, *Fuel*, 2010, **89**, 2713–2720.

60 R. L. Bechtold, *Alternative Fuels Guidebook: Properties, Storage, Dispensing, and Vehicle Facility Modifications [R-180]*, Society of Automotive Engineers Inc., 2014.

61 P. Roy, R. Roy and B. K. Mandal, *Int. J. Sci. Eng. Res.*, 2013, **4**(12), 986–989.

62 Ricardo Inc., *Impact of Vehicle Weight Reduction on Fuel Economy for Various Vehicle Architectures*, 2008.

63 F. H. Palmer, *Vehicle Performance of Gasoline Containing Oxygenates. International Conference on Petroleum Based Fuels and Automotive Applications (IMechE Conference Publications 1986-11)*, Society of Automotive Engineers Inc, 1986.

64 M. Z. Bardaie and R. Janius, *Ama, Agric. Mech. Asia, Afr. Lat. Am.*, 1984, 31–34.

65 Green Car Congress, *DOE Co-Funds 12 Projects to Increase Engine Efficiency*, 2005.

66 J.-P. Lange, *Catal. Today*, 2001, **64**, 3–8.

67 K. A. Ali, A. Z. Abdullah and A. R. Mohamed, *Renewable Sustainable Energy Rev.*, 2015, **44**, 508–518.

68 A. Riaz, G. Zahedi and J. J. Klemeš, *J. Cleaner Prod.*, 2013, **57**, 19–37.

69 S. Wasmus and A. Küver, *J. Electroanal. Chem.*, 1999, **461**, 14–31.

70 N. Radenahmad, A. Afif, P. I. Petra, S. M. Rahman, S.-G. Eriksson and A. K. Azad, *Renewable Sustainable Energy Rev.*, 2016, **57**, 1347–1358.

71 I. Ganesh, *Renewable Sustainable Energy Rev.*, 2014, **31**, 221–257.

72 S. G. Jadhav, P. D. Vaidya, B. M. Bhanage and J. B. Joshi, *Chem. Eng. Res. Des.*, 2014, **92**, 2557–2567.

73 W.-H. Wang, Y. Himeda, J. T. Muckerman, G. F. Manbeck and E. Fujita, *Chem. Rev.*, 2015, **115**, 12936–12973.

74 K. Li, X. An, K. H. Park, M. Khraisheh and J. Tang, *Catal. Today*, 2014, **224**, 3–12.

75 A. Iulianelli, P. Ribeirinha, A. Mendes and A. Basile, *Renewable Sustainable Energy Rev.*, 2014, **29**, 355–368.

76 S. Yong, C. Ooi, S. Chai and X. Wu, *Int. J. Hydrogen Energy*, 2013, **38**, 9541–9552.

77 E. Aransiola, T. Ojumu, O. Oyekola, T. Madzimbamuto and D. Ikuh-Omoregbe, *Biomass Bioenergy*, 2014, **61**, 276–297.

78 B. Bharathiraja, M. Chakravarthy, R. R. Kumar, D. Yuvaraj, J. Jayamuthunagai, R. P. Kumar and S. Palani, *Renewable Sustainable Energy Rev.*, 2014, **38**, 368–382.

79 X. Zhen and Y. Wang, *Renewable Sustainable Energy Rev.*, 2015, **52**, 477–493.

80 A. Elfasakhany, *Int. J. Eng. Sci. Technol.*, 2015, **18**, 713–719.

81 I. Yusri, R. Mamat, G. Najafi, A. Razman, O. I. Awad, W. Azmi, W. Ishak and A. Shaiful, *Renewable Sustainable Energy Rev.*, 2017, **77**, 169–181.

82 P. Tian, Y. Wei, M. Ye and Z. Liu, *ACS Catal.*, 2015, **5**, 1922–1938.

83 K. Hemelsoet, J. Van der Mynsbrugge, K. De Wispelaere, M. Waroquier and V. Van Speybroeck, *ChemPhysChem*, 2013, **14**, 1526–1545.

84 A. Galadima and O. Muraza, *J. Nat. Gas Sci. Eng.*, 2015, **25**, 303–316.

85 Z. Wan, W. Wu, W. Chen, H. Yang and D. Zhang, *Ind. Eng. Chem. Res.*, 2014, **53**, 19471–19478.

86 M. Saito, T. Fujitani, M. Takeuchi and T. Watanabe, *Appl. Catal., A*, 1996, **138**, 311–318.

87 É. S. Van-Dal and C. Bouallou, *J. Cleaner Prod.*, 2013, **57**, 38–45.

88 M. Pérez-Fortes, J. C. Schöneberger, A. Boulamanti and E. Tzimas, *Appl. Energy*, 2016, **161**, 718–732.

89 D. Milani, R. Khalilpour, G. Zahedi and A. Abbas, *J. CO₂ Util.*, 2015, **10**, 12–22.

90 The Secretary of Energy Advisory Board (SEAB) CO₂ Utilization Task Force, *Task Force on RD&D strategy for CO₂ Utilization and/or Negative Emissions at the gigatonne scale, U.S. Department of Energy technical report*, 2016.



91 WindEurope, *WindEurope views on curtailment of wind power and its link to priority dispatch*, 2016.

92 Office of Gas and Electricity Markets, *Electricity interconnectors*, <https://www.ofgem.gov.uk/electricity/transmission-networks/electricity-interconnectors>, 2017.

93 Department for Transport, *Table ENV0501. Volume of fuels by fuel type: United Kingdom*, 2016.

94 Department for Transport, *Table VEH0150. Vehicles registered for the first time by body type, Great Britain, monthly: January 2001 to June 2015, Vehicle Licensing Statistics*, 2015.

95 Department for Transport, *Table NTS0901. Annual mileage of 4-wheeled cars by ownership and trip purpose: England, 2002 to 2016, National Travel Survey 2016*, 2016.

96 J. Artz, T. E. Müller, K. Thenert, J. Kleinekorte, R. Meys, A. Sternberg, A. Bardow and W. Leitner, *Chem. Rev.*, 2017, **118**(2), 434–504.

97 EIRGRID and SONI, *Annual Renewable Energy Constraint and Curtailment Report 2015*, 2016.

98 Bundesnetzagentur, *EEG in Zahlen 2015-Inhaltsverzeichnis*, 2016.

99 J. M. Douglas, *Conceptual Design of Chemical Processes*, McGraw-Hill, 1988.

100 U.S. Energy Information Administration, *Levelised Cost and Levelized Avoided Cost of New Generation Resources in the Annual Energy Outlook 2016*, 2016.

101 E. S. Rubin, J. E. Davison and H. J. Herzog, *Int. J. Greenhouse Gas Control*, 2015, **40**, 378–400.

102 B. Bonner, *Current Hydrogen Cost, DOE Hydrogen and Fuel Cell Technical Advisory Committee*, 2013, https://www.hydrogen.energy.gov/pdfs/htac_oct13_10_bonner.pdf, accessed on 26-01-2018.

103 G. Collodi, G. Azzaro, N. Ferrari and S. Santos, *Energy Procedia*, 2017, **114**, 2690–2712.

104 Office of Energy Efficiency and Renewable Energy, *Multi-Year Research, Development, and Demonstration Plan*, 2015.

105 Methanex, *Methanex posts regional contract methanol prices for North America, Europe and Asia*, 2017.

106 Global Carbon Capture and Storage Institute Ltd, *The Costs of CCS and Other Low-Carbon Technologies in the United States - 2015 Update*, 2015.

107 Gerhard Beysel - The Linde Group, *1st Oxyfuel Combustion Conference*, 2009.

108 A. Ebrahimi, M. Meratizaman, H. A. Reyhani, O. Pourali and M. Amidpour, *Energy*, 2015, **90**, 1298–1316.

109 I. Sharafutdinov, S. Dahl and I. Chorkendorff, Ph.D. thesis, Department of Physics, Technical University of Denmark, 2013.

110 A. Cybulski, *Catal. Rev.*, 1994, **36**, 557–615.

111 N. J. Brown, J. Weiner, K. Hellgardt, M. S. P. Shaffer and C. K. Williams, *Chem. Commun.*, 2013, **49**, 11074–11076.

112 B. Li and K.-J. Jens, *Ind. Eng. Chem. Res.*, 2014, **53**, 1735–1740.

113 A. Bansode and A. Urakawa, *J. Catal.*, 2014, **309**, 66–70.

114 A. Álvarez, A. Bansode, A. Urakawa, A. V. Bavykina, T. A. Wezendonk, M. Makkee, J. Gascon and F. Kapteijn, *Chem. Rev.*, 2017, **117**, 9804–9838.

115 N. von der Assen, J. Jung and A. Bardow, *Energy Environ. Sci.*, 2013, **6**, 2721–2734.

116 V. Arutyunov, *Direct Methane to Methanol*, Elsevier Science & Technology, 2014.

117 A. Holmen, *Catal. Today*, 2009, **142**, 2–8.

118 M. Alvarez-Galvan, N. Mota, M. Ojeda, S. Rojas, R. Navarro and J. Fierro, *Catal. Today*, 2011, **171**, 15–23.

119 R. A. Periana, D. J. Taube, E. R. Evitt, D. G. Löffler, P. R. Wentreek, G. Voss and T. Masuda, *Science*, 1993, **259**, 340–343.

120 J. Liao, L. Mi, S. Pontrelli and S. Luo, *Nat. Rev. Microbiol.*, 2016, **14**, 288–304.

121 B. Michalkiewicz, *Appl. Catal., A*, 2004, **277**, 147–153.

122 C. Kalamaras, D. Palomas, R. Bos, A. Horton, M. Crimmin and K. Hellgardt, *Catal. Lett.*, 2016, **146**, 483–492.

